Assembly of ROMK1 (Kir 1.1a) Inward Rectifier K^+ Channel Subunits Involves Multiple Interaction Sites

Joseph C. Koster,* Kristin A. Bentle,# Colin G. Nichols,* and Kevin Ho#

*Department of Cell Biology and Physiology and #Renal Division and Department of Medicine, Washington University School of Medicine, St. Louis, Missouri 63110 USA

ABSTRACT The ROMK1 (Kir 1.1a) channel is formed by a tetrameric complex of subunits, each characterized by cytoplasmic N- and C-termini and a core region of two transmembrane helices flanking a pore-forming segment. To delineate the general regions mediating the assembly of ROMK1 subunits we constructed epitope-tagged N-terminal, C-terminal, and transmembrane segment deletion mutants. Nonfunctional subunits with N-terminal, core region, and C-terminal deletions had dominant negative effects when coexpressed with wild-type ROMK1 subunits in *Xenopus* oocytes. In contrast, coexpression of these nonfunctional subunits with Kv 2.1 (DRK1) did not suppress Kv 2.1 currents in control oocytes. Interactions between epitope-tagged mutant and wild-type ROMK1 subunits were studied in parallel by immunoprecipitating [^{35}S]-labeled oocyte membrane proteins. Complexes containing both wild-type and mutant subunits that retained H5, M2, and C-terminal regions were coimmunoprecipitated to a greater extent than complexes consisting of wild-type and mutant subunits with core region and/or C-terminal deletions. The present findings are consistent with the hypothesis that multiple interaction sites located in the core region and cytoplasmic termini of ROMK1 subunits mediate homomultimeric assembly.

INTRODUCTION

Inwardly rectifying K^+ channels contribute to the stabilization of the resting membrane potential and the modulation of cell excitability. Members of this family include classical inward rectifiers, G-protein-gated muscarinic K^+ channels, ATP-sensitive K^+ channels, and epithelial ATP-regulated K^+ channels that underlie physiologically important currents including I_{K1}, I_{KACh}, and I_{KATP}, as well as K^+ secretory pathways in epithelial cells. These channels are characterized by a reduction in conductance at depolarizing potentials; rectification results from the voltage-dependent block of the channel pore by intracellular Mg^{2+} and positively charged polyamines (Vandenberg, 1987; Matsuda et al., 1987; Nichols et al., 1994; Stanfield et al., 1994; Lopatin et al., 1994; Ficker et al., 1994; Fakler et al., 1995).

Reflecting the functional heterogeneity of inward rectifiers, six subfamilies of inwardly rectifying potassium channel genes (Kir 1.0–Kir 6.0) have been identified that are expressed in various cell types, including neurons, cardiac myocytes, pancreatic β-cells, and renal epithelial cells (Doupnik et al., 1995; Nichols and Lopatin, 1997; Ho, 1998). An additional level of structural diversity is generated by the coassembly of Kir channel subunits in a restricted manner either within a subfamily or between subfamilies to give rise to functional heteromultimeric channels with distinct properties. For example, within the Kir 3.0 subfamily Kir 3.1 and Kir 3.4 coassemble to form G-protein-gated muscarinic K^+ channels in cardiac atria (Krapivinsky et al., 1995); subunits from the same subfamily also form heteromultimeric neuronal channels (Lesage et al., 1995). Intersubfamily heteromultimers (e.g., Kir 1.1/Kir 4.1) have also been reported (Glowatzki et al., 1995).

As with voltage-gated K^+ (Kv) channels, heterologous expression studies support a tetrameric structure for Kir channels in which each subunit of the tetramer contributes to the formation of a central ion-conducting pore (Glowatzki et al., 1995; Yang et al., 1995; Clement et al., 1997; Shyng and Nichols, 1997). Structurally, however, Kir channel subunits display a distinct membrane topology. Hydropathy and sequence analyses predict cytoplasmic N- and C-termini with a core region that consists of two transmembrane segments, M1 and M2, flanking a pore-forming H5 segment (Ho et al., 1993).

A full understanding of Kir channel quaternary structure, assembly, and mechanisms determining the specificity of subunit multimerization requires knowledge of the regions involved in subunit interactions. Domains with a role in Kir channel heteromultimerization and homomultimerization have been proposed based largely on the ability of chimeric subunits to associate with and alter wild-type channel activity. Fink et al. (1996) suggested that the Kir 2.3 N-terminus functions as a requisite structural element in both homomultimeric and heteromultimeric (Kir 2.1/Kir 2.3) assembly events and that the Kir 3.2 core region confers an inactive channel phenotype on Kir 2.0/Kir 3.2 heteromultimeric channels. In the same context, Tucker et al. (1996a) have identified the two putative transmembrane segments of Kir 3.4 as conferring an inhibitory interaction of this subunit on heteromultimers formed with Kir 4.1. The M1 and M2 segments also have been shown to mediate the potentiated currents in Kir 3.1/Kir 3.4 heteromultimeric channels (Kubo and Iizuka, 1996; Tucker et al., 1996b). On the other hand, chimeric and deletion analysis studies by Tinker et al.

Received for publication 30 September 1997 and in final form 30 December 1997.

Address reprint requests to Dr. Kevin Ho, Washington University School of Medicine, Renal Division, Box 8126, 660 South Euclid Avenue, St. Louis, MO 63110. Tel.: 314-362-4309; Fax: 314-362-8237; E-mail: kho@imgate.wustl.edu.

0006-3495/98/04/1821/09 $2.00

(1996) have implicated a distal C-terminal segment in homomultimeric subunit association and the M2 transmembrane segment and a proximal C-terminal region in restricting heteromultimeric channel assembly. These data suggest that a single common structural motif may not mediate Kir assembly, in contrast to the major role of the NAB domain in Kv channel assembly (Li et al., 1992; Shen et al., 1993; Hopkins et al., 1994; Xu et al., 1995). Specific roles for each of these putative domains in subunit association and/or in determining the specificity of heteromultimeric subunit interactions are yet unresolved.

In the present study we have examined the homomultimerization of ROMK1 (Kir 1.1a) (Ho et al., 1993) channel subunits heterologously expressed in *Xenopus laevis* oocytes to delineate general regions that directly mediate Kir channel assembly. Mutations in the Kir 1.1 gene (*KCNJ1*) result in the disorder, Bartter's syndrome (Simon et al., 1996). ROMK1 N-terminal, C-terminal, and core region deletion mutants were generated and coexpressed with wild-type channel proteins. Parallel functional and biochemical assays demonstrated specific association of mutants with full-length ROMK1 subunits in vivo. These data support a model for homomultimerization in which adjacent channel subunits of the ROMK1 tetramer interact at multiple sites of association distributed within the cytoplasmic N-terminal, C-terminal, and transmembrane core regions of each subunit. A preliminary report of these findings has been presented to the Biophysical Society (Koster et al., 1997).

MATERIALS AND METHODS

Electrophysiology

Expression of ROMK1 mutant and wild-type channel subunits in Xenopus *oocytes*

cRNA was transcribed in vitro using T7 or SP6 RNA polymerase (Ambion Corp., Austin, TX), and additional purification of cRNAs was performed using G-50 Sephadex RNA spin columns (Boehringer-Mannheim, Indianapolis, IN). Stage V–VI *Xenopus laevis* oocytes were isolated by partial ovariectomy under tricaine anesthesia and defolliculated by treatment with 1 mg/ml type 1A collagenase (Sigma, St. Louis, MO) in ND96 solution [96 mM NaCl, 2 mM KCl, 1 mM $MgCl_2$, 5 mM Na-HEPES (pH 7.5)] for 1 h. Oocytes were microinjected with ~50 nl cRNA (1–100 ng/μl) 24 h to 48 h after defolliculation. Oocytes were maintained at 22°C in ND96 solution with 2 mM Ca^{2+}, penicillin (100 U/ml), and streptomycin (100 μg/ml) for 1–2 days before recording. Two-electrode voltage clamp recordings were obtained using an OC-725C amplifier (Warner Instruments, Hamden, CT). In any given batch of oocytes, uninjected oocytes never had conductances >1 μS. Expressed currents were leak-subtracted using mean currents recorded from three to six mock-injected oocytes. Data were recorded and analyzed using a chart recorder, an Axon TL-1 A/D interface, and pClamp 5.5 software (Axon Instruments, Foster City, CA). Currents were recorded in KD98 solution [98 mM KCl, 1 mM $MgCl_2$, 5 mM K-HEPES (pH 7.5)] unless otherwise indicated.

Molecular biology

Construction of deletion mutants

Cassette-based mutagenesis techniques combining standard and inverse PCR were used to incorporate HA (influenza hemagglutinin I) or T7 (T7 major capsid protein) epitopes into the N- and C-terminal ends of ROMK1, respectively, using rTth DNA polymerase, XL (Perkin-Elmer, Foster City, CA). After PCR mutagenesis, restriction fragments containing epitope sequences were subcloned back into ROMK1-pSPUTK to generate the tagged full-length constructs ROMK1-N-HA and ROMK1-C-T7. With ROMK1-N-HA as a PCR template, construction of the deletion mutants, ΔN1, ΔN2, ΔM1, ΔM2, ΔC1 and ΔC2, applied inverse PCR mutagenesis using oligonucleotide primers that incorporated either *Nde*I or *Xho*I restriction endonuclease sites for recircularization. The more complex deletion mutants, ΔN3, ΔN2C2, ΔM1H5M2, ΔN2M1, and ΔH5M2C2, were generated by combining restriction fragments derived from the above constructs and by PCR mutagenesis. By using a cassette strategy to minimize secondary mutations, restriction endonuclease fragments containing the deletion mutations from all constructs incorporating PCR-generated regions were subcloned back into ROMK1-N-HA to generate mutants with N-terminal HA epitope tags. The nucleotide sequences of all constructs were verified by double-stranded sequencing using Sequenase 2.0 T7 DNA polymerase (USB Speciality Biochemicals, Cleveland, OH) or fluorescence-based cycle sequencing using AmpliTaq DNA polymerase, FS (Perkin-Elmer, Foster City, CA) and an ABI PRISM DNA sequencer (Perkin-Elmer, Foster City, CA).

Metabolic labeling of *Xenopus* oocytes

cRNAs encoding epitope-tagged full-length and deletion mutant constructs were microinjected into oocytes (~15–30 ng cRNA per oocyte). After injection oocytes were incubated for ~12 h at 18°C in ND96 solution with 2 mM Ca^{2+}. Healthy oocytes were selected and labeled with 74 MBq/ml [^{35}S]methionine/[^{35}S]cysteine (Dupont New England Nuclear, Boston, MA) in ND96 solution (+2 mM Ca^{2+}, penicillin/streptomycin) for 12–14 h at 18°C. After labeling, oocytes were transferred to homogenization buffer [10 mM HEPES, 250 mM sucrose, and protease inhibitor cocktail (Boehringer-Mannheim, Indianapolis, IN) (pH 7.4)] and homogenized at 4°C. The homogenate was centrifuged three times (10 min, 1000 × *g*) at 4°C to remove yolk granules and melanosomes. The resulting supernatant was ultracentrifuged at 165,000 × *g* for 45 min at 4°C to generate a total membrane fraction that was used for the immunoprecipitation assay described below.

Immunoprecipitation of ROMK1 mutant and full-length channel subunits

Total membrane pellets from injected oocytes were washed with STE buffer containing 1 M NaCl, 50 mM Tris, 1 mM EDTA (pH 7.9) (10 min, 15,000 × *g*) followed by a second wash using buffer without NaCl at 4°C. Membranes were solubilized in buffer containing 1% Triton X-100, 1% sodium deoxycholate, 0.5% SDS, 150 mM NaCl, 50 mM Tris, 1 mM EDTA (pH 7.9) supplemented with protease inhibitor cocktail for 15 min at 4°C and diluted in a stepwise fashion with STE buffers to a final detergent concentration of 0.5% Triton X-100, 0.5% sodium deoxycholate, and 0.05% SDS. After centrifugation (10 min, 15,000 × *g*), supernatants were transferred to new microcentrifuge tubes. To immunoprecipitate epitope-tagged channel subunits, two 200-μl aliquots taken from the same solubilized membrane protein preparation were incubated at 4°C with either anti-T7 monoclonal antibody (0.01 μg/μl) (Novagen, Madison, WI) or anti-HA 12CA5 monoclonal antibody (0.02 μg/μl) (Boehringer-Mannheim, Indianapolis, IN) followed by the addition of Protein G Sepharose (Pharmacia Biotech, Piscataway, NJ). Immunoprecipitates were pelleted (1 min, 15,000 × *g*) and washed sequentially five times (5 min, 4°C) with the following wash buffers: 1) 0.5% Triton X-100, 0.5% sodium deoxycholate, 0.05% SDS in 150 mM NaCl-STE (pH 7.9) (3 washes); 2) 0.05% Triton X-100, 0.05% sodium deoxycholate, 0.005% SDS in 500 mM NaCl-STE (pH 7.9) (1 wash); and 3) 0.05% Triton X-100, 0.05% sodium deoxycholate, 0.005% SDS in STE buffer without NaCl (pH 7.9) (1 wash). Immunoprecipitated proteins were eluted in SDS Laemmli sample buffer with 5% β-mercaptoethanol and proteins were separated by SDS-PAGE; 10% or 10–20% gradient SDS-PAGE gels were used depend-

ing on the mutant proteins resolved. Gels were incubated in fixative (10% acetic acid, 25% isopropanol) for 30 min at 25°C followed by an additional 15 min (25°C) in fluorographic reagent (Amersham, Arlington Heights, IL) before fluorography.

Quantitation of immunoprecipitated mutant and wild-type subunits

In order to compare the relative efficiency of coprecipitating mutant and wild-type subunits, we calculated $R_{coprecip}$ (Eq. 1) for each group of paired immunoprecipitations resulting from a given membrane protein preparation. Relative quantities of mutant and full-length subunits in immunoprecipitates were determined by densitometry using SigmaGel software (SPSS Inc., Chicago, IL) following resolution of proteins by SDS-PAGE and fluorography. Glycosylated and unglycosylated forms were quantitated separately but the densitometric data were combined for the following calculations. $R_{coprecip}$ relates the quantities of coprecipitated protein and immunoprecipitated protein while adjusting for the number of methionine residues present in each:

$$R_{coprecip} = [C/M_c]/[I/M_I] \quad (1)$$

where I is the protein (with M_I number of methionine residues) directly immunoprecipitated by antibody and C is the protein (with M_c number of methionine residues) coprecipitated. Since the absolute amounts of mutant and full-length subunit proteins present in membrane preparations could not be determined before immunoprecipitations, we assumed that HA-tagged mutant and T7-tagged full-length subunit proteins were expressed to different extents in coinjected oocytes resulting in an excess of one subunit type over the other. An approximation of coprecipitation efficiency might then be obtained by selecting the higher of the two values for $R_{coprecip}$ determined from both anti-T7 and anti-HA immunoprecipitations of each membrane protein preparation. The higher $R_{coprecip}$ value would correspond to the immunoprecipitation of the subunit type present in a limiting quantity (as opposed to the subunit type in relative excess) resulting in a better estimate; in contrast, the lower of the two $R_{coprecip}$ values would be consistent with the immunoprecipitation of the subunit type in relative excess resulting in an underestimate of coprecipitation efficiency. For this reason, the higher of the two $R_{coprecip}$ values generated for each group of paired immunoprecipitations is given.

RESULTS

Expression of ROMK1 epitope-tagged deletion mutant and wild-type subunits in *Xenopus* oocytes

We generated N-terminal, C-terminal, and core region deletion mutants in order to delineate the general region(s) involved in the homomultimeric assembly of ROMK1 channel subunits (Fig. 1). Constructs encoding deletion mutant and full-length (wild-type) ROMK1 proteins incorporated N-terminal HA (influenza hemagglutinin I) or C-terminal T7 (T7 major capsid protein) epitopes, respectively, to provide the means to specifically isolate each subunit type. When expressed alone in *Xenopus* oocytes, HA-tagged mutants with deletions involving the C-terminus (ΔC1, ΔC2), N-terminus (ΔN2), transmembrane segment-containing core region (ΔM2, ΔM1H5M2), or a combination of these regions (ΔN2C2, ΔN2M1, ΔH5M2C2) did not generate functional channels (Fig. 2). However, a mutant with a partial deletion of the N-terminus, ΔN1 (residues 3–38), was functional; currents were similar but larger in magnitude when compared to those associated with wild-type subunits [ROMK1 = 5.5 ± 0.4 μA (n = 10); ΔN1 = 12.1 ± 1.2 μA (n = 9) (+50 mV)].

Inactive mutant subunits function as dominant negative subunits when coexpressed with ROMK1 in oocytes

To demonstrate the involvement of general subunit regions in homomultimerization, we coexpressed the nonfunctional mutants with full-length subunits in *Xenopus* oocytes and looked for current suppression (dominant negative effect). Coexpression of mutant subunits with the very distantly related voltage-gated K^+ (Kv) channel, Kv 2.1 (DRK1) (Frech et al., 1989), was used in parallel groups of oocytes as a control for nonspecific effects associated with the expression of multiple proteins in oocytes and for nonspecific protein-protein interactions. Current evidence supports the notion that Kv and Kir channel subunits do not coassemble with each other to form heteromultimeric channels (Tytgat et al., 1996; Tinker et al., 1996). In comparison to the currents recorded from oocytes expressing wild-type subunits alone, the coexpression of mutant and wild-type subunits resulted in significant suppression of ROMK1 currents (Figs. 3 and 4). This interaction between mutant and full-length ROMK1 subunits was specific: there was no

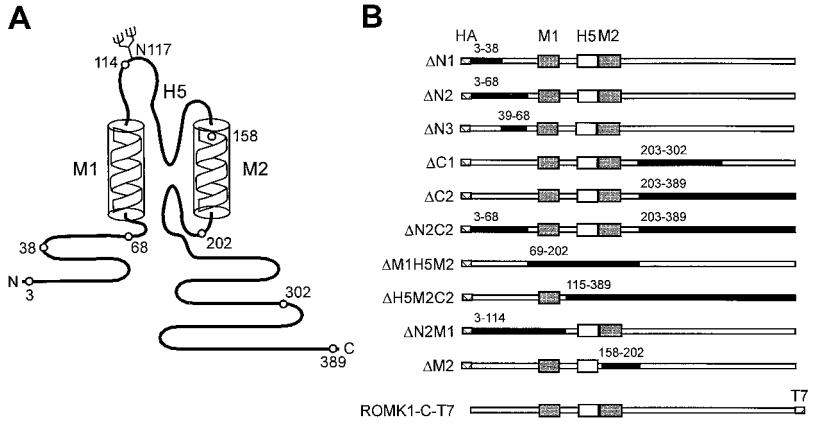

FIGURE 1 Epitope-tagged ROMK1 (Kir1.1a) deletion mutant and wild-type subunits. (*A*) Schematic of the Kir 1.1a channel subunit illustrating the general topology of Kir channel subunits. Residues delineating deleted segments are indicated. (*B*) HA (influenza hemagglutinin) and T7 (T7 major capsid protein) epitopes were respectively incorporated into the N- and C-termini of deletion mutant and wild-type ROMK1 constructs as shown using cassette-based PCR mutagenesis. Addition of either epitope tag did not significantly alter ROMK1 channel function (data not shown). For each deletion mutant construct residues corresponding to deleted segments (*black regions*) are indicated above. The expected size of each polypeptide was confirmed by in vitro translating each construct using a rabbit reticulocyte lysate system (Promega, Madison, WI) followed by SDS-PAGE (data not shown).

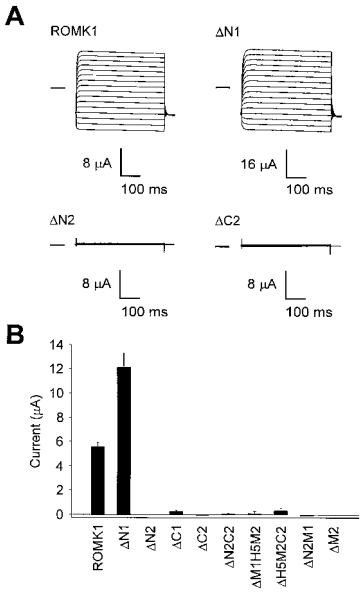

FIGURE 2 Expression of ROMK1 and deletion mutant subunits in *Xenopus* oocytes. (*A*) Representative whole-cell currents recorded from *Xenopus* oocytes injected with equimolar amounts of cRNA encoding ROMK1 or mutant channel proteins using two-electrode voltage clamp. Currents were elicited by test potentials between −80 mV and +70 mV in 10-mV increments from a holding potential of −50 mV. Bath solution contained 98 mM KCl, 1 mM $MgCl_2$, 5 mM K-HEPES (pH 7.5). (*B*) Mean leak-subtracted currents at −50 mV recorded from oocytes expressing mutant subunits alone compared with ROMK1 currents in control oocytes. Bars indicate S.E.M. (n = 3–10 oocytes/group).

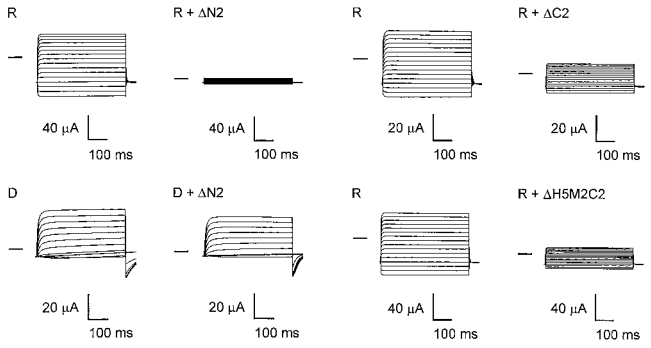

FIGURE 3 N-terminal, C-terminal, and core region deletion mutants function as dominant negative subunits when coexpressed with ROMK1 in oocytes. Representative whole-cell currents recorded by two-electrode voltage clamp from oocytes expressing ROMK1 subunits (R) alone or coexpressing both wild-type and mutant subunits (R + mutant); ROMK1: mutant cRNA ratio for coinjected oocytes was 1:1 or 1:3. To demonstrate the specificity of the interaction between wild-type and mutant subunits, each deletion construct was also coexpressed with voltage-gated K^+ channel Kv 2.1 (DRK1) subunits (D) in oocytes (from the same batch used for ROMK1 studies) and compared to oocytes expressing Kv 2.1 alone. The amount of mutant cRNA coinjected with Kv 2.1 cRNA in these oocytes was equivalent to that used in coinjection experiments with ROMK1. Currents were recorded in KD98 solution and elicited by test potentials between −80 mV and +70 mV in 10-mV increments from a holding potential of −50 mV.

significant difference in the magnitudes of Kv 2.1 currents recorded from control oocytes expressing Kv 2.1 channels alone and from control oocytes coexpressing mutant and Kv 2.1 subunits (Table 1).

Mutant subunits with deletions of the N-terminus (ΔN2), C-terminus (ΔC1, ΔC2), or both (ΔN2C2) reduced wild-type channel activity. The mutant subunit, ΔN2 (residues 3–68), had the most marked inhibitory effect on ROMK1 currents. The reduction in currents associated with a more limited deletion of the N-terminus, ΔN3 (residues 39–68), was comparable (data not shown). Common to each of these subunit constructs is retention of the core region, M1-H5-M2, therefore suggesting a role for this region in homomultimerization.

Dominant negative effects were not limited only to mutants possessing an intact core region, however. A mutant with a complete deletion of the core region, ΔM1H5M2, was also able to suppress wild-type channel activity; the finding is consistent with the presence of interaction site(s) within the putative cytoplasmic N- and C-termini. Suppression of ROMK1 currents by ΔH5M2C2, which consists of only the N-terminus and M1 transmembrane segment, provides evidence for an interaction site(s) within these regions. Moreover, the reduction in wild-type currents by ΔN2M1 suggests at least one additional site of interaction in the remaining half of the subunit (H5-M2-C-terminus).

Immunoprecipitation of [^{35}S]-labeled mutant and wild-type subunits from oocytes

In an effort to better understand the mechanism(s) underlying these suppressive effects, we examined whether some or all of the dominant negative effects reflect the formation of stable complexes consisting of mutant and wild-type subunits. *Xenopus* oocytes coexpressing T7-tagged wild-type ROMK1 (ROMK1-C-T7) and HA-tagged mutant subunits (cRNA molar ratio, 1:3) were metabolically labeled in [^{35}S]methionine/[^{35}S]cysteine-containing media. Oocyte

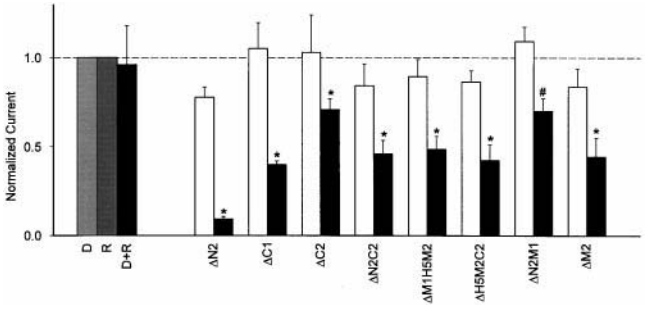

FIGURE 4 Mean leak-subtracted currents from oocytes coexpressing mutant subunits and either ROMK1 (−50 mV, *black bars*) or Kv 2.1 (+50 mV, *white bars*) as shown in Fig. 3 were normalized to mean currents from oocytes expressing ROMK1 (R) alone or Kv 2.1 (DRK1) (D) alone using the same batch of oocytes. Coexpression of ROMK1 and Kv 2.1 (D + R). Normalized, mean leak-subtracted currents from coinjected oocytes, R + mutant or D + mutant, were statistically compared to currents from oocytes expressing either ROMK1 or Kv 2.1 alone, respectively, using unpaired t-tests; $P < 0.0005$–0.05 (*asterisk*) and $P < 0.07$ (*pound sign*). Bars indicate S.E.M. (n = 3–14 oocytes/group).

TABLE 1 Coexpression of deletion mutant subunits and wild-type ROMK1 or Kv 2.1 subunits in *Xenopus* oocytes

ROMK1			Kv 2.1		
Oocyte Group	Mean Normalized Current ± S.E. (*n*)	ROMK1 vs. ROMK1 + Mutant	Oocyte Group	Mean Normalized Current ± S.E. (*n*)	Kv 2.1 vs. Kv 2.1 + Mutant
ROMK1	1.000 ± 0.129 (4)		Kv 2.1	1.000 ± 0.118 (6)	
ROMK1 + ΔN2	0.092 ± 0.014 (6)	$P < 0.0005$	Kv 2.1 + ΔN2	0.777 ± 0.057 (10)	NS
ROMK1	1.000 ± 0.086 (9)		Kv 2.1	1.000 ± 0.078 (8)	
ROMK1 + ΔC1	0.398 ± 0.022 (8)	$P < 0.0005$	Kv 2.1 + ΔC1	1.051 ± 0.144 (10)	NS
ROMK1	1.000 ± 0.079 (9)		Kv 2.1	1.000 ± 0.141 (11)	
ROMK1 + ΔC2	0.708 ± 0.061 (14)	$P < 0.05$	Kv 2.1 + ΔC2	1.029 ± 0.211 (12)	NS
ROMK1	1.000 ± 0.102 (3)		Kv 2.1	1.000 ± 0.145 (9)	
ROMK1 + ΔN2C2	0.459 ± 0.076 (6)	$P < 0.005$	Kv 2.1 + ΔN2C2	0.842 ± 0.123 (6)	NS
ROMK1	1.000 ± 0.135 (13)		Kv 2.1	1.000 ± 0.110 (11)	
ROMK1 + ΔM1H5M2	0.484 ± 0.073 (11)	$P < 0.005$	Kv 2.1 + ΔM1H5M2	0.894 ± 0.096 (11)	NS
ROMK1	1.000 ± 0.083 (10)		Kv 2.1	1.000 ± 0.050 (10)	
ROMK1 + ΔH5M2C2	0.423 ± 0.087 (8)	$P < 0.0005$	Kv 2.1 + ΔH5M2C2	0.864 ± 0.064 (7)	NS
ROMK1	1.000 ± 0.117 (8)		Kv 2.1	1.000 ± 0.169 (7)	
ROMK1 + ΔN2M1	0.700 ± 0.072 (6)	NS*	Kv 2.1 + ΔN2M1	1.093 ± 0.081 (6)	NS
ROMK1	1.000 ± 0.174 (14)		Kv 2.1	1.000 ± 0.169 (9)	
ROMK1 + ΔM2	0.443 ± 0.107 (13)	$P < 0.05$	Kv 2.1 + ΔM2	0.837 ± 0.101 (9)	NS

Mean leak-subtracted currents recorded from *Xenopus* oocytes coinjected with ROMK1 and mutant cRNAs were normalized and compared to currents recorded from oocytes expressing ROMK1 alone (at −50 mV). Currents were also recorded from control oocytes (from the same oocyte batch) coexpressing Kv 2.1 (DRK1) and mutant constructs; these were normalized and compared to currents recorded from oocytes expressing Kv 2.1 alone (at +50 mV). Statistical analyses were performed with SigmaPlot software (SPSS Inc., Chicago, IL.) using unpaired *t*-tests; significance was defined by a P value < 0.05. NS, not significant.

* Note that for ΔN2M1, ROMK1 alone vs. ROMK1 + ΔN2M1, $P < 0.07$; in control oocytes, Kv 2.1 alone vs. Kv 2.1 + ΔN2M1, $P > 0.6$.

membranes were isolated and detergent-solubilized (1% Triton X-100 + 1% sodium deoxycholate + 0.5% SDS), and the resulting membrane proteins were immunoprecipitated using monoclonal antibodies directed against the T7 epitope (ROMK1-C-T7 subunit) or HA epitope (mutant subunit).

Representative detergent-solubilized [^{35}S]-labeled oocyte membrane proteins (*lanes 1–3*), antibody specificity controls, and paired immunoprecipitations (both anti-T7 and anti-HA) from a single representative experiment are shown for the mutant, ΔN1 (Fig. 5). As controls, ROMK1-C-T7 and mutant subunits were specifically immunoprecipitated by anti-T7 (compare *lanes 5* and *6*) and anti-HA (compare *lanes 9* and *10*) monoclonal antibodies, respectively, from oocytes expressing each subunit type alone and without the precipitation of endogenous oocyte proteins. No detectable cross-reactivity was observed between anti-T7 antibody and HA-tagged subunits or between anti-HA antibody and T7-

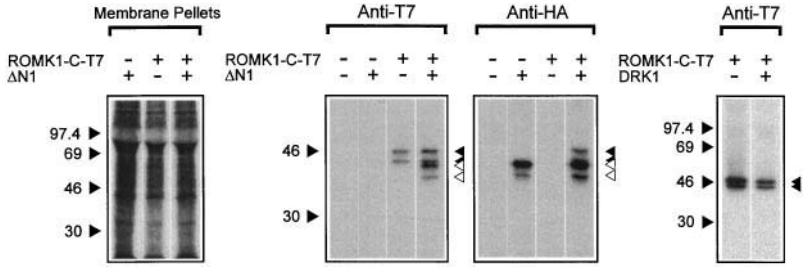

FIGURE 5 Immunoprecipitation of mutant (N-terminal HA-tagged) and wild-type (ROMK1-C-T7) subunits expressed in *Xenopus* oocytes. Equal aliquots of total detergent-solubilized [^{35}S]-labeled membrane proteins isolated from each group of oocytes were immunoprecipitated using anti-T7 and anti-HA monoclonal antibodies (paired immunoprecipitations) and resolved by SDS-PAGE. Representative detergent-solubilized membrane proteins from oocytes expressing ΔN1, ROMK1-C-T7, or both (ROMK1:mutant cRNA ratio, 1:3) resolved by SDS-PAGE (10% gel) before immunoprecipitation (*lanes 1–3*). Solubilized total membrane proteins were immunoprecipitated using anti-T7 and anti-HA monoclonal antibodies, and immunoprecipitates were resolved on a 10% SDS-PAGE gel (*lanes 4–11*). Anti-T7 antibody immunoprecipitated only ROMK1-C-T7 and not ΔN1 (*lanes 5* and *6*). Conversely, anti-HA antibody immunoprecipitated only ΔN1 and not ROMK1-C-T7 (*lanes 9* and *10*). However, both ΔN1 and ROMK1-C-T7 subunits were coimmunoprecipitated from oocytes coexpressing both subunit types using either anti-T7 (*lane 7*) or anti-HA (*lane 11*) monoclonal antibodies demonstrating the coassembly of these subunits. Endogenous oocyte proteins were not immunoprecipitated; in addition, no proteins were immunoprecipitated from mock-injected oocytes (*lanes 4* and *8*). Migrating as doublets, glycosylated and unglycosylated forms of ROMK1-C-T7 (*black arrows on right*) and ΔN1 subunits (*white arrows on right*) were expressed in oocytes as previously shown for wild-type ROMK1 (Ho et al., 1993; Schwalbe et al., 1995) and clearly resolved by 10% SDS-PAGE gel. Immunoprecipitation of membrane proteins from oocytes coexpressing Kv 2.1 (95.3 kDa predicted size) and ROMK1-C-T7 subunits using anti-T7 antibody yielded only ROMK1-C-T7 subunits (*lane 13*); glycosylated and unglycosylated ROMK1-C-T7 subunits were observed to migrate closely on 10–20% gradient SDS-PAGE gels.

tagged ROMK1. Immunoprecipitation of membrane proteins isolated from oocytes expressing both ROMK1-C-T7 and Kv 2.1 channels using anti-T7 antibody resulted in only the precipitation of ROMK1-C-T7 subunits.

A stable, direct interaction between functional ΔN1 and ROMK1-C-T7 subunits was demonstrated in oocytes coexpressing the two subunit types. Both HA-tagged ΔN1 and ROMK1-C-T7 subunits were coprecipitated when either anti-T7 or anti-HA monoclonal antibodies were used to specifically immunoprecipitate each subunit type, thus demonstrating a physical interaction between the subunits (*lanes 7* and *11*). Paired immunoprecipitations were used in these studies to demonstrate the identities of the proteins involved and the specificity of the interactions. Appearing as doublets, glycosylated and unglycosylated forms of ΔN1 and ROMK1-C-T7 were present in the immunoprecipitates in agreement with previous reports for ROMK1 (Ho et al., 1993; Schwalbe et al., 1995) and GIRK1 (Kir 3.1) subunits (Dascal et al., 1995).

Mutant subunits retaining both core and C-terminal regions coprecipitate with wild-type subunits to the greatest extent

In addition to the functionally active ΔN1 mutant, nonfunctional mutant subunits that exhibited a dominant negative effect on the expression of wild-type currents also specifically coprecipitated with ROMK1-C-T7, but with significant differences in efficiency (Figs. 6 and 7). Paired immunoprecipitations resulted in the isolation of stable complexes consisting of ROMK1-C-T7 and mutant subunits retaining the H5, M2, and C-terminal regions (ΔN1, ΔN2, ΔN2M1) from coinjected oocytes. In contrast, immunoprecipitations of complexes containing both ROMK1-C-T7 and mutant subunits with deletions involving the entire C-terminus (ΔC2, ΔN2C2) and/or core region [ΔM1H5M2, ΔH5M2C2, ΔM2, and ΔM1 (residues 69–114) (data not shown for the latter two mutants)] were consistently of low efficiency, yielding mainly the primary precipitated species. The coprecipitation of ROMK1-C-T7 and ΔC1 was of intermediate efficiency; ROMK1-C-T7 was coprecipitated by ΔC1 (containing the distal C-terminal segment, 303–391) to a greater extent than by ΔC2 as shown by immunoprecipitations using anti-HA antibody (Fig. 6). Quantitative comparison of the relative efficiency of coprecipitating mutant and ROMK1-C-T7 subunits was made by calculating $R_{coprecip}$ (see Materials and Methods) for each group of paired immunoprecipitations shown in Figs. 5 and 6. Higher values reflect a greater efficiency of coprecipitation: ΔN1 1.11; ΔN2 0.63; ΔN2M1 0.89; ΔC1 0.37; ΔC2 0.02; ΔN2C2 0.04; ΔM1H5M2 0.13; ΔH5M2C2 0.06. Interactions occurred between ROMK1-derived subunits and not with labeled endogenous membrane proteins, which represented the vast majority of labeled proteins (note the SDS-PAGE separations of representative preparations of solubilized membrane proteins before immunoprecipitation; Fig. 5, *lanes 1–3*). Both glycosylated and unglycosylated forms of the mutants, ΔN2, ΔC1, ΔC2, ΔN2C2, and ΔN2M1, were present in the immunoprecipitates and are consistent with the single N-linked glycosylation site present in the M1-H5 linker (Asn-117). These biochemical data suggest that the simultaneous presence of H5, M2, and C-terminal regions confer a greater stability on ROMK1 subunit interactions than do the N-terminus and core region.

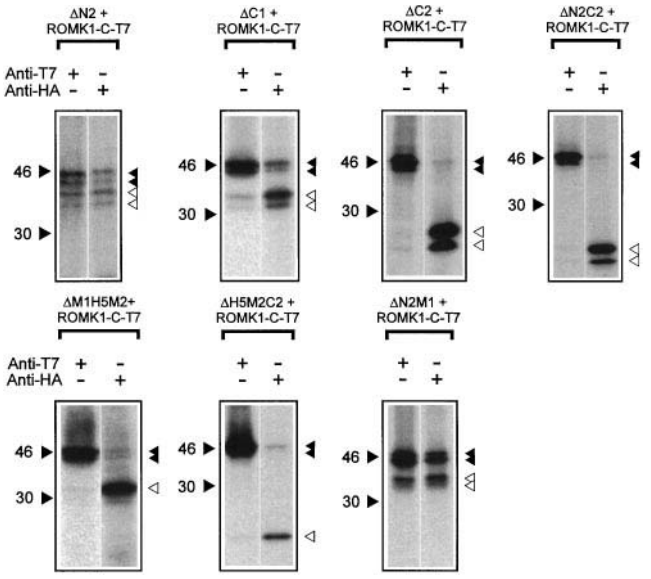

FIGURE 6 Functionally inactive deletion mutants were coexpressed with ROMK1-C-T7 in oocytes and immunoprecipitated with anti-T7 and anti-HA monoclonal antibodies as in Fig. 5. Immunoprecipitates were resolved by SDS-PAGE as follows: 10% gel, ΔN2; 10–20% gradient gel, ΔC1, ΔC2, ΔN2C2, ΔM1H5M2, ΔH5M2C2, ΔN2M1. Glycosylated and unglycosylated forms of ROMK1-C-T7 (*black arrows on right*) and mutant subunits (*white arrow*(*s*) *on right*) are indicated (in the latter case, if present). The ROMK1-C-T7 doublet, which is difficult to discern in some 10–20% gradient gel lanes due to longer exposure times, was easily visualized in each of these cases by using shorter exposures (data not shown). Faint, lower-molecular-weight bands visible in some lanes most likely represent degradation products. Predicted sizes of subunit proteins: ROMK1-C-T7, 46.3 kDa; ΔN1 41.8, kDa; ΔN2, 38.4 kDa; ΔC1, 35.4 kDa; ΔC2, 25.3 kDa; ΔN2C2, 17.4 kDa; ΔM1H5M2, 31.2 kDa; ΔN2M1, 32.6 kDa; ΔH5M2C2, 15.7 kDa.

DISCUSSION

The ROMK1 (Kir 1.1a) channel consists of a tetramer of four noncovalently associated subunits forming a central K^+-selective aqueous pore (Glowatzki et al., 1995; Yang et al., 1995). To begin to define the structural determinants involved in the homomultimerization of these channels, a series of deletion mutant subunits was constructed and assayed for the ability to specifically associate with wild-type subunits in *Xenopus* oocytes using both functional and biochemical approaches. There has been relatively little characterization of the molecular or subcellular mechanisms responsible for the functional phenotypes (suppression or activation) associated with the interaction of heterologously

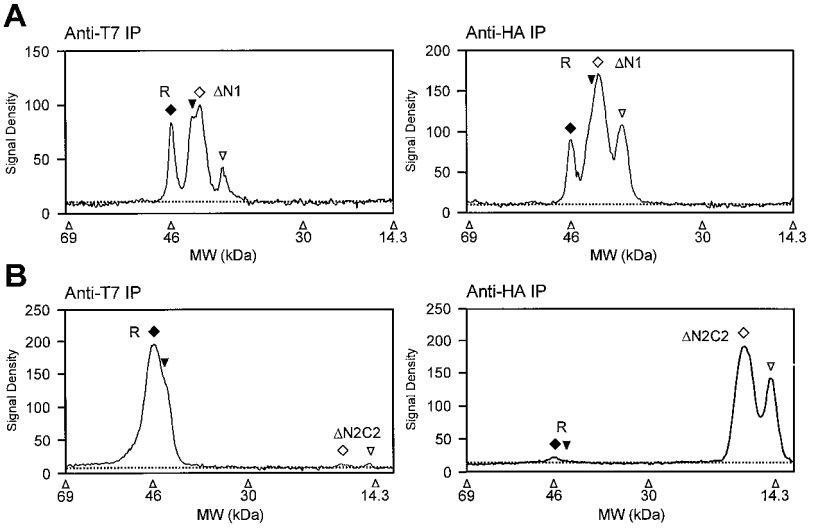

FIGURE 7 Quantitation of mutant and wild-type subunits in immunoprecipitates. ROMK1-C-T7 and mutant subunits, which were immunoprecipitated using anti-T7 and anti-HA monoclonal antibodies and resolved by SDS-PAGE (Figs. 5 and 6), were quantitated by densitometry. Representative densitometric traces are shown for paired immunoprecipitations of ΔN1 (*A*) and ΔN2C2 (*B*) coexpressed with ROMK1-C-T7. For both full-length (*filled symbols*) and mutant (*open symbols*) subunits, the corresponding positions of both glycosylated (*diamonds*) and unglycosylated (*inverted triangles*) forms are indicated. Mutant subunits retaining both core and C-terminal regions coprecipitated with wild-type subunits to a greater extent. $R_{coprecip}$ was calculated for each group of paired immunoprecipitations as an alternative means of demonstrating the relative efficiency of coprecipitating mutant and ROMK1-C-T7 subunits (see text).

expressed Kir channel subunits. Using a homotypic system we have demonstrated that the oligomerization of ROMK1 subunits involves multiple interaction sites distributed along the length of the Kir channel polypeptide, in contrast to the central role of the N-terminal NAB assembly domain in voltage-gated K^+ channels. Differences in the interactions identified by dominant negative and immunoprecipitation assays suggest that channel suppression may be mediated by different mechanisms.

Studies that have examined the assembly of Kir channels primarily through the analysis of chimeric subunit interactions have identified different regions involved in subunit association. The N-terminus (Fink et al., 1996), the transmembrane segments, M1 and M2 (Tucker et al., 1996a,b; Kubo and Iizuka, 1996), as well as M2 and C-terminal regions (Tinker et al., 1996) have been implicated in oligomerization as assembly domains, specificity domains (providing a recognition mechanism for discriminating between compatible and incompatible subunit interactions), or domains with both of these functions. We chose to investigate the oligomerization of a single Kir subfamily member, ROMK1, in an attempt to separate the issue of subunit compatibility (heteromultimerization) from the issue of subunit association. The present study, which focuses on purely homotypic interactions between ROMK1 subunit proteins expressed in *Xenopus* oocytes, provides evidence that more than one site contributes to intersubunit interactions. In agreement, Woodward et al. (1997) have recently shown that multiple determinants in Kir 3.1 play a role in the assembly of G-protein-gated Kir channels.

Mutant subunits with deletions of the N- and/or C-terminus (ΔN2, ΔN3, ΔC1, ΔC2, ΔN2C2), but which retain the core region, suppressed wild-type ROMK1 currents in coinjected oocytes. These data are consistent with an interaction between the core region present in these mutants and wild-type subunits. Similarly, a chimeric protein consisting of the Kir 3.1 core and Kir 2.1 N-terminal regions has been found to associate with full-length Kir 3.1 and Kir 3.2 (Woodward et al., 1997). Designation of the Kir core region as an assembly domain would be consistent with the inhibitory effects conferred by the incorporation of Kir 3.1, Kir 3.2, or Kir 3.4 core regions (specifically, transmembrane segments M1 and M2) into heteromultimeric channels that have been reported by others (Fink et al., 1996; Tucker et al., 1996a). Similarly, Kir 3.4/Kir 2.1 and Kir 3.1/Kir 4.1 chimeric constructs have been used to demonstrate that the Kir 3.0 core region is necessary for the potentiation of currents observed with Kir 3.1/Kir 3.4 heteromultimers (Kubo and Iizuka, 1996; Tucker et al., 1996b). By analogy, in voltage-gated K^+ channels, Tu et al. (1996) have reported that in addition to the N-terminal NAB domain (Li et al., 1992; Shen et al., 1993; Hopkins et al., 1994; Xu et al., 1995) and S1 transmembrane segment (Babila et al., 1994) which were previously identified as determinants of Kv channel assembly, regions within the Kv 1.3 channel core region (transmembrane segments S1–S6) also facilitate intersubunit association (Tu et al., 1996).

The dominant negative effect of the core-region mutant, ΔM1H5M2, on ROMK1 currents in oocytes coexpressing mutant and wild-type subunits suggests that additional interaction sites exist in the N-terminus and/or C-terminus. In fact, we found that mutant subunits consisting either of the N-terminus and M1 transmembrane segment (ΔH5M2C2) or the remaining half of ROMK1 inclusive of the H5-M2-C-terminus regions (ΔN2M1) suppressed wild-type currents. Taken together, these results are consistent with an interaction of N- and C-terminal domains with wild-type subunits. In agreement, subunit constructs corresponding to the Kir 3.1 N-terminus, N-terminus-M1 regions, and C-terminus have been reported to compete with full-length Kir 3.1 in coassembling with Kir 3.2 (Woodward et al., 1997). Furthermore, a Kir 3.1 C-terminal peptide inhibited G-protein-gated K^+ currents when coexpressed with wild-type subunits in oocytes (Dascal et al., 1995). Chimeric studies have also shown that N-terminal (Kir 2.3) (Fink et al., 1996) and C-terminal regions (Kir 1.0 and Kir 2.0) (Tinker et al., 1996) can independently restrict the compatibility of heteromultimeric subunit oligomerization.

Coimmunoprecipitation of mutant and wild-type ROMK1 subunits is evidence for a specific and direct interaction. Paired immunoprecipitations (using anti-T7 and anti-HA monoclonal antibodies) were performed to confirm the identity of each interacting protein and to demonstrate the specificity of the subunit interactions studied; two different monoclonal antibodies directed against either the T7-tagged full-length subunit or the HA-tagged mutant subunits yielded immunoprecipitates containing the same protein species (ROMK1-C-T7 and mutant) from common preparations of solubilized oocyte membrane proteins. No significant precipitation of endogenous oocyte proteins was detectable as assessed by paired immunoprecipitations of membrane proteins from control oocytes expressing only mutant subunits or ROMK1-C-T7 subunits. The specificity of these immunoprecipitation experiments therefore complements the absence of a significant inhibitory effect of mutant subunits on Kv 2.1 currents in control oocytes.

An intriguing finding was the observation that dominant negative effects did not directly correlate with the efficient isolation of mutant/wild-type subunit complexes by immunoprecipitation. The efficiency of coprecipitating ROMK1-C-T7 and N-terminal mutants retaining H5, M2, and C-terminal regions (ΔN1, ΔN2, ΔN2M1) was significantly greater than that for isolating complexes consisting of full-length and mutant subunits with C-terminal (ΔC2) and/or core region (ΔM1H5M2, ΔH5M2C2) deletions. Moreover, ΔC1, which retains the distal C-terminal segment 303–391 in addition to H5 and M2 segments, coprecipitated with ROMK1-C-T7 to a greater extent than mutants with deletions of this segment (ΔC2, ΔN2C2, ΔH5M2C2).

These biochemical results suggest that mutant subunits retaining the H5, M2, and distal C-terminal regions form complexes with wild-type subunits that are more stable than subunits retaining only the N-terminus and/or core region, perhaps by exhibiting greater resistance to degradation in vivo and/or to dissociation under the detergent/ionic conditions utilized in vitro. The strong dominant negative effects exhibited by ΔN2 and ΔN3 are consistent with this possibility. Deletions of the core region (ΔM1H5M2), the distal C-terminus (ΔC2, ΔN2C2), or both (ΔH5M2C2) might then be expected to result in a reduction in mutant/wild-type subunit complexes isolated. This does not account, however, for the small effect of ΔN2M1 despite its significant coprecipitation with ROMK1-C-T7; the result could reflect a difference in the number of ΔN2M1 subunits required to render a channel complex nonfunctional. Although we cannot currently distinguish among the various possibilities, the distinct results yielded by the functional and biochemical approaches highlight likely differences in the stability of these subunit interactions, assembly and membrane-trafficking of multimers, and efficiency of mutant subunits in knocking-out channel activity.

Potential mechanisms for channel suppression by mutant subunits include the formation of nonfunctional channels or channels with reduced activity, sequestration of nascent wild-type monomers, retention of subunit complexes in the endoplasmic reticulum, and increased degradation of multimeric complexes. While the first three mechanisms may yield subunit complexes that can be isolated by immunoprecipitation (Tu et al., 1996; Kennedy et al., 1996), dominant negative effects resulting from the fourth mechanism have been associated with decreases in the detectable levels of the interacting subunits (Tucker et al., 1996a; Tinker et al., 1996). The suppression of Kir 4.1 (BIR 10) currents by the coexpression of Kir 3.0 (Kir 3.1, Kir 3.2, Kir 3.4) in oocytes results from the degradation of Kir 3.0/Kir 4.1 heteromultimers; Kir 4.1 subunits were undetectable by immunoblot analysis (Tucker et al., 1996a). Similarly, the levels of detectable interacting subunits resulting in Kir 2.1 current suppression were reduced in HEK293 cells cotransfected with Kir 2.1 and chimeric Kir 6.1/Kir 2.1 (Tinker et al., 1996). The degradation of heteromultimeric complexes in vivo may therefore contribute to the apparent weak coprecipitation of wild-type and mutant ROMK1 subunits with core region and C-terminal deletions.

A deletion analysis strategy to identify determinants of subunit assembly is potentially constrained by the topology of the expressed deletion mutants. A reduction in subunit association could reflect improper folding, presentation, or sequestration of an interaction site rather than its absence. It is notable, then, that ROMK1 deletion mutants that retain the solitary N-linked glycosylation site at Asn-117 (ΔN1, ΔN2, ΔC1, ΔC2, ΔN2C2, ΔM2, ΔN2M1) migrate as doublets on SDS-PAGE gels consistent with both glycosylated and unglycosylated forms in agreement with prior studies, while mutants in which the sequence has been deleted (ΔM1H5M2, ΔH5M2C2) migrate as solitary bands. Since no other glycosylation motifs exist in the ROMK1 subunit, glycosylation of a mutant polypeptide topologically constrains the region containing Asn-117 to the endoplasmic reticulum lumen and the extracellular space. The observation that ΔM1H5M2 fractionates with membranes implicates membrane-anchoring sites in the cytoplasmic termini. The binding of ROMK1 N- and C-terminal peptides to phospholipid membranes has been reported (Ben-Efraim and Shai, 1996). Recently, Schwalbe et al. (1997) have proposed a novel Kir channel topology based on N-glycosylation sequon substitution mutations in ROMK1 in which the putative cytoplasmic C-terminus contains two additional membrane-associated segments.

In summary, studies of voltage-gated K^+ (Kv) channel assembly have characterized an N-terminal domain, NAB, with a major role in mediating Kv subunit interactions. By comparison, recent studies of Kir channel assembly have provided independent evidence supporting the involvement of different regions (transmembrane segments, cytoplasmic termini) in Kir heteromultimerization and homomultimerization. The combined biochemical and electrophysiological analyses of ROMK1 (Kir 1.1a) subunit interactions in the present study together with those of G-protein-gated Kir (Kir 3.0) channels (Woodward et al., 1997) suggest a common assembly pattern for Kir channel

subunits involving not a single region but multiple interaction sites in the core region and cytoplasmic termini.

We thank Q. Sha for oocyte preparations and A. Permutt and J. Wasson for their assistance in DNA sequencing. DRK1 cDNA was a gift from Rolf Joho, U.T.S.W. Dallas. We are grateful to R. Mercer and J. Lytton for discussion and critical comments.

This work was supported by National Institutes of Health Grants HL451231 and HL54171 (to C.G.N.), and DK02389 (to K.H.); an Established Investigatorship from the American Heart Association (to C.G.N.), and a National Institutes of Health DRTC Training Grant Fellowship (to J.C.K.).

REFERENCES

Babila, T., A. Moscucci, H. Wang, F. E. Weaver, and G. Koren. 1994. Assembly of mammalian voltage-gated potassium channels: evidence for an important role of the first transmembrane segment. *Neuron*. 12:615–626.

Ben-Efraim, I., and Y. Shai. 1996. Secondary structure, membrane localization, and coassembly within phospholipid membranes of synthetic segments derived from the N- and C-termini regions of the ROMK1 K^+ channel. *Protein Sci.* 5:2287–2297.

Clement, J. P. IV, K. Kunjilwar, G. Gonzalez, M. Schwanstecher, U. Panten, L. Aguilar-Bryan, and J. Bryan. 1997. Association and stoichiometry of K_{ATP} channel subunits. *Neuron.* 18:827–838.

Dascal, N., C. A. Doupnik, T. Ivanina, S. Bausch, W. Wang, C. Lin, J. Garvey, C. Chavkin, H. A. Lester, and N. Davidson. 1995. Inhibition of function in *Xenopus* oocytes of the inwardly rectifying G-protein-activated atrial K channel (GIRK1) by overexpression of a membrane-attached form of the C-terminal tail. *Proc. Natl. Acad. Sci. USA.* 92: 6758–6762.

Doupnik, C. A., N. Davidson, and H. A. Lester. 1995. The inward rectifier potassium channel family. *Curr. Opin. Neurobiol.* 5:268–277.

Fakler, B., U. Brändle, E. Glowatzki, S. Weidemann, H.-P. Zenner, and J. P. Ruppersberg. 1995. Strong voltage-dependent inward rectification of inward rectifier K^+ channels is caused by intracellular spermine. *Cell.* 80:149–154.

Ficker, E., M. Taglialatela, B. A. Wible, C. M. Henley, and A. M. Brown. 1994. Spermine and spermidine as gating molecules for inward rectifier K^+ channels. *Science.* 266:1068–1072.

Fink, M., F. Duprat, C. Heurteaux, F. Lesage, G. Romey, J. Barhanin, and M. Lazdunski. 1996. Dominant negative chimeras provide evidence for homo and heteromultimeric assembly of inward rectifier K^+ channel proteins via their N-terminal end. *FEBS Lett.* 378:64–68.

Frech, G. C., A. M. J. VanDongen, G. Schuster, A. M. Brown, and R. H. Joho. 1989. A novel potassium channel with delayed rectifier properties isolated from rat brain by expression cloning. *Nature.* 340:642–645.

Glowatzki, E., G. Fakler, U. Brändle, U. Rexhausen, H.-P. Zenner, J. P. Ruppersberg, and B. Fakler. 1995. Subunit-dependent assembly of inward-rectifier K^+ channels. *Proc. R. Soc. Lond. B.* 261:251–261.

Ho, K. 1998. The ROMK-CFTR connection (new insights into the relationship between ROMK and CFTR channels). *Curr. Opin. Nephrol. Hypertension.* 7:49–58.

Ho, K., C. G. Nichols, W. J. Lederer, J. Lytton, P. M. Vassilev, M. V. Kanazirska, and S. C. Hebert. 1993. Cloning and expression of an inwardly rectifying ATP-regulated potassium channel. *Nature.* 362:31–38.

Hopkins, W. F., V. Demas, and B. L. Tempel. 1994. Both N- and C-terminal regions contribute to the assembly and functional expression of homo- and heteromultimeric voltage-gated K^+ channels. *J. Neurosci.* 14:1385–1393.

Kennedy, M. E., J. Nemec, and D. E. Clapham. 1996. Localization and interaction of epitope-tagged GIRK1 and CIR inward rectifier K^+ channel subunits. *Neuropharmacol.* 35:831–839.

Koster, J. C., K. A. Bentle, C. G. Nichols, and K. Ho. 1997. Homomeric assembly of ROMK1 channels via distinct domains in the C-terminal cytoplasmic region and transmembrane segments. *Biophys. J.* 72:254*a*. (Abstr.).

Krapivinsky, G., E. A. Gordon, K. Wickman, B. Velimirovic, L. Krapivinsky, and D. E. Clapham. 1995. The G-protein-gated atrial K^+ channel I_{KACh} is a heteromultimer of two inwardly rectifying K^+ channel proteins. *Nature.* 374:135–141.

Kubo, Y., and M. Iizuka. 1996. Identification of domains of the cardiac inward rectifying K^+ channel, CIR, involved in the heteromultimer formation and in the G-protein gating. *Biochem. Biophys. Res. Commun.* 227:240–247.

Lesage, F., E. Guillemare, M. Fink, F. Duprat, C. Heurteaux, M. Fosset, G. Romey, J. Barhanin, and M. Lazdunski. 1995. Molecular properties of neuronal G-protein-activated inwardly rectifying K^+ channels. *J. Biol. Chem.* 270:28660–28667.

Li, M., Y. N. Jan, and L. Y. Jan. 1992. Specification of subunit assembly by the hydrophilic amino-terminal domain of the *Shaker* potassium channel. *Science.* 257:1225–1230.

Lopatin, A. N., E. N. Makhina, and C. G. Nichols. 1994. Potassium channel block by cytoplasmic polyamines as the mechanism of intrinsic rectification. *Nature.* 372:366–369.

Matsuda, H., A. Saigusa, and H. Irisawa. 1987. Ohmic conductance through the inwardly rectifying K^+ channel and blocking by internal Mg^{2+}. *Nature.* 325:156–159.

Nichols, C. G., K. Ho, and S. Hebert. 1994. Mg^{2+}-dependent inward rectification of ROMK1 potassium channels expressed in *Xenopus* oocytes. *J. Physiol.* 476:399–409.

Nichols, C. G., and A. N. Lopatin, 1997. Inward rectifier potassium channels. *Annu. Rev. Physiol.* 59:171–191.

Schwalbe, R. A., L. Bianchi, and A. M. Brown. 1997. Mapping the kidney potassium channel ROMK1. Glycosylation of the pore signature sequence and the COOH terminus. *J. Biol. Chem.* 272:25217–25223.

Schwalbe, R. A., Z. Wang, B. A. Wible, and A. M. Brown. 1995. Potassium channel structure and function as reported by a single glycosylation sequon. *J. Biol. Chem.* 270:15336–15340.

Shen, N. V., X. Chen, M. M. Boyer, and P. J. Pfaffinger. 1993. Deletion analysis of K^+ channel assembly. *Neuron.* 11:67–76.

Shyng, S.-L., and C. G. Nichols. 1997. Octameric stoichiometry of the K_{ATP} channel complex. *J. Gen. Physiol.* 110:655–664.

Simon, D. B., F. E. Karet, J. Rodriguez-Soriano, J. H. Hamdan, A. Dipietro, H. Trachtman, S. A. Sanjad, and R. P. Lifton. 1996. Genetic heterogeneity of Bartter's syndrome revealed by mutations in the K^+ channel, ROMK. *Nature Genet.* 14:152–156.

Stanfield, P. R., N. W. Davies, P. A. Shelton, I. A. Khan, W. J. Brammar, N. B. Standen, and E. C. Conley. 1994. The intrinsic gating of inward rectifier K^+ channels expressed from the murine IRK1 gene depends on voltage, K^+ and Mg^{2+}. *J. Physiol.* 475:1–7.

Tinker, A., Y. N. Jan, and L. Y. Jan. 1996. Regions responsible for the assembly of inwardly rectifying potassium channels. *Cell.* 87:857–868.

Tu, L., V. Santarelli, Z. Sheng, W. Skach, D. Pain, and C. Deutsch. 1996. Voltage-gated K^+ channels contain multiple intersubunit association sites. *J. Biol. Chem.* 271:18904–18911.

Tucker, S. J., C. T. Bond, P. Herson, M. Pessia, and J. P. Adelman. 1996a. Inhibitory interactions between two inward rectifier K^+ channel subunits mediated by the transmembrane domains. *J. Biol. Chem.* 271: 5866–5870.

Tucker, S. J., M. Pessia, and J. P. Adelman. 1996b. Muscarine-gated K^+ channel: subunit stoichiometry and structural domains essential for G protein stimulation. *Am. J. Physiol.* 271: H379–H385.

Tytgat, J., G. Buyse, J. Eggermont, G. Droogmans, B. Nilius, and P. Daenens. 1996. Do voltage-gated Kv1.1 and inward rectifier Kir2.1 potassium channels form heteromultimers? *FEBS Lett.* 390:280–284.

Vandenberg, C. A. 1987. Inward rectification of a potassium channel in cardiac ventricular cells depends on internal magnesium ions. *Proc. Natl. Acad. Sci. USA.* 84:2560–2562.

Woodward, R., E. B. Stevens, and R. D. Murrell-Lagnado. 1997. Molecular determinants for assembly of G-protein-activated inwardly rectifying K^+ channels. *J. Biol. Chem.* 272:10823–10833.

Xu, J., W. Yu, Y. N. Jan, L. Y. Jan, and M. Li. 1995. Assembly of voltage-gated potassium channels. *J. Biol. Chem.* 270:24761–24768.

Yang, J., Y. N. Jan, and L. Y. Jan. 1995. Determination of the subunit stoichiometry of an inwardly rectifying potassium channel. *Neuron.* 15:1441–1447.